ORIGINAL PAPER

Facile preparation Pt on Au dendrites supported on Si (100) and their electrochemical properties for methanol and CO electrooxidation

Yanling Zhang · Hao Tong · Zhipeng Sun ·
Sudong Yang · Zhuliang Wen · Jiajia Zhu · Liang Hao ·
Yongqin Han · Xiaogang Zhang

Abstract A new simple, time-saving method of preparing highly dispersed Pt nanoparticles with large electrochemically active area (ECA) on three-dimensional dendrite-like Au supported on Si (100) was successfully developed by electroless displacement deposition (EDD). The as-prepared catalysts were characterized by field-emission scanning electron microscope and high-resolution transmission electron microscopy. The electro-catalytic properties of Pt/Au/Si for methanol and CO electrooxidation were investigated by cyclic voltammetry, chronoamperometry, and electrochemical impedances spectra. The results show that Pt/Au/Si catalyst prepared by EDD method presents the higher electro-catalytic activity and higher stability than that of Pt/Si composite. The electro-catalytic activity of Pt supported on Au could be enhanced with the growth of Au, leading to the higher electro-catalytic properties toward methanol and CO oxidation. The anodic peak of CO of Pt/Au/Si catalyst showed negatively shifted with respect to similarly prepared Pt/Si electrode. The supposed schematic of the reaction was also introduced. Overall, the approach provides a convenient method to prepare the Pt

catalyst on Au dendrites with high ECA properties for DMFC and PEMFC through bottom-up assembly.

Introduction

Recently, synthesis of nanostructures of metal particles with high electrochemically active area (ECA) has attracted much attention in the field of fuel cell catalysts [1]. Among all the catalytic metals, Pt possesses the exclusive chemical and physical properties for electro-catalytic oxidation of small organic molecules such as methanol and formic acid [2, 3]. However, Pt is expensive due to the limited supply and the preparation of Pt nanoparticles is difficult and time-consuming. To enhance the catalytic activity and reduce the cost of catalysts, it would be necessary to decrease the particle size of Pt and keep the loading of catalysts as low as possible. One of the best ways to achieve this goal is to manufacture the high electro-catalytic area such as Pt particles supported on 3D large surface network rendering the reactants diffusion channels and enough adsorption sites for reactant molecules over a close range [4, 5]. Dendritic Au nanostructure possessing the high-specific surface area can be prepared due to its potential application in thermal, optical, chemical, and physical properties [6]. Additionally, the silicon support with good conductivity and stability was found very suitable for catalyst supporter. Tiwari et al. have used the electrodeposition to fabricate the two-dimensional Pt network and 3D Pt nanoflowers on Si [5, 7]. However, how to reduce the high loading of Pt without losing the high catalytic activity still needs further investigation.

Y. Zhang · H. Tong (✉) · S. Yang · Z. Wen · J. Zhu · L. Hao ·
Y. Han · X. Zhang (✉)
College of Material Science and Technology,
Nanjing University of Aeronautics and Astronautics,
Nanjing 210016, China
e-mail: tongh@nuaa.edu.cn

X. Zhang
e-mail: azhangxg@163.com

Z. Sun
Department of Chemical and Biomolecular Engineering,
National University of Singapore,
Singapore 117576, Singapore

Among various methods of preparing metal islands on semiconductors, electroless displacement deposition (EDD) is an attractive way due to its low-processing temperature, low cost, time-saving, and simplicity. We have developed electrodeposition and EDD methods to prepare the metal seed layer on silicon [8]. Additionally, various kinds of metals such as Cu, Au, Ag, Pt, Rh have been deposited on silicon by this method with the solution containing fluoride and metal salts [8–13]. Dendritic gold structures used as surface enhancement Raman scattering active substrates can also be prepared by this method [6].

The lower distribution and high aggregation of Pt particles on silicon prepared by EDD method, however, could not easily obtain the excellent electrochemical and photoelectrochemical activities [9]. Although Shao et al. [14] have reported the Pt/Si electrode could serve as the ethanol electrooxidation electrode, the preparation of Pt/Si still needs high K_2PtCl_6 concentration of 0.01 M with regular freshness solution during plating, not favoring for the low loading of Pt catalyst.

To date, no research regarding the Pt deposited on dendrite-like Au supported on Si by EDD method serving as the high activity and stable electro-catalytic catalyst has been reported. In this paper, we introduce the facile way, including two EDD steps, to fabricate the stable Pt/Au/Si catalyst. Firstly, the etched silicon wafer was dipped into the solution containing $HAuCl_4$/HF for some time to obtain the dendritic Au on silicon surface, then the prepared Au/Si wafer was immersed into the solution containing H_2PtCl_6/HF to gain the Pt/Au/Si. The prepared Pt/Au/Si catalysts were tested as electrocatalysts for the methanol and CO electrooxidation. The result show that Pt particles can be distributed on dendritic Au surface in the H_2PtCl_6/HF solution with higher electro-catalytic activity and excellent stability in acid solution. The electro-catalytic properties of Pt/Au/Si toward methanol and CO oxidation could be enhanced with the growth of Au dendrites. In brief, it may have potential application in commercialization for preparing anodic material of DMFC and PEMFC (proton exchange membrane fuel cell).

Experimental

Wafer treatment and preparation of Pt/Au/Si electrode

The fabrication steps of Pt/Au/Si are described as follows: The pretreatment of Si (100) wafer is the same as our previous works [7]. The activation of preparing Au dendrites on Si was performed by introducing the etched Si wafer into the solution containing 4.4×10^{-3} or 8.8×10^{-4} M $HAuCl_4$/9.1 M HF for 10 or 30 min at room temperature. After that, the prepared Au/Si electrode was dipped into the

3.5×10^{-3} M H_2PtCl_6/9.1 M HF solution also at room temperature for 10 min to fabricate Pt/Au/Si. By comparison, the Pt/Si catalyst was prepared by dipping etched Si in 3.5×10^{-3} M H_2PtCl_6/9.1 M HF solution for 10 min.

Characterization

Electrochemical experiments were performed by CHI 750 electrochemical workstation (Chenhua, Shanghai). The electrochemical measurements were made with three-electrode cell at 25 °C. Pt foil and saturated calomel electrode (SCE) were used as the counter and reference electrodes, respectively. The microscopic features of the sample were observed with a field-emission scanning electron microscope (FESEM, LEO-1550) and high-resolution transmission electron microscopy (HR-TEM; JEM-2100). Energy-dispersive X-ray analyzer (EDX, Quanta 2000) was used to determine the metal mass fraction of catalysts.

A home-made electrochemical cell was used to measure the electrochemical measurements [15]. All mentioned potential in this paper refer to the SCE. The as-prepared silicon electrode was used as working electrode. All experiment was carried out at room temperature.

Results and discussion

Surface morphology of the Pt, Au, and Pt/Au on silicon by EDD preparation was investigated by scanning electron microscopy (SEM), respectively. Fig. 1a shows images of silicon (100) after immersion into H_2PtCl_6/HF solution for 10 min. The Pt particles are distributed sparsely with the particles size between 50 and 300 nm. The density of Pt particles remains constantly except for the gradual growth of particle size with the increase of deposition time. Yae et al. [9] have classified electroless displacement reaction on silicon into two types of nucleation behavior. One is progressive growth model, including Pt, Rh, Pd, leading the lower density of particle on silicon. The other is instantaneous mode, consisting of Cu, Ag, and Au, showing the higher density than that of progressive growth model. Accordingly, it is very difficult to prepare high density of Pt particles with high ECA on Si by EDD method, owing to the progressive growth mode of Pt on silicon. While, the Au particles can instantly form the condensed nuclei on Si surface in the case of the deposition of Si wafer into $HAuCl_4$/HF electroless solution. Compared with Pt particles on silicon in Fig. 1b, the Au particles could also grow larger, almost covering the substrate with the increase of dipping time. After deposition for 10 min, the Au particles with the size

between 100 and 400 nm could be observed. Interestingly, there are still some slits and voids between the Au particles, which will cause the following oxidation of Si by HF, leading to further metal deposition. The dendrites of Au can be formed with the increase of deposition time. As shown in Fig. 1c, d, it can be clearly seen in the high magnific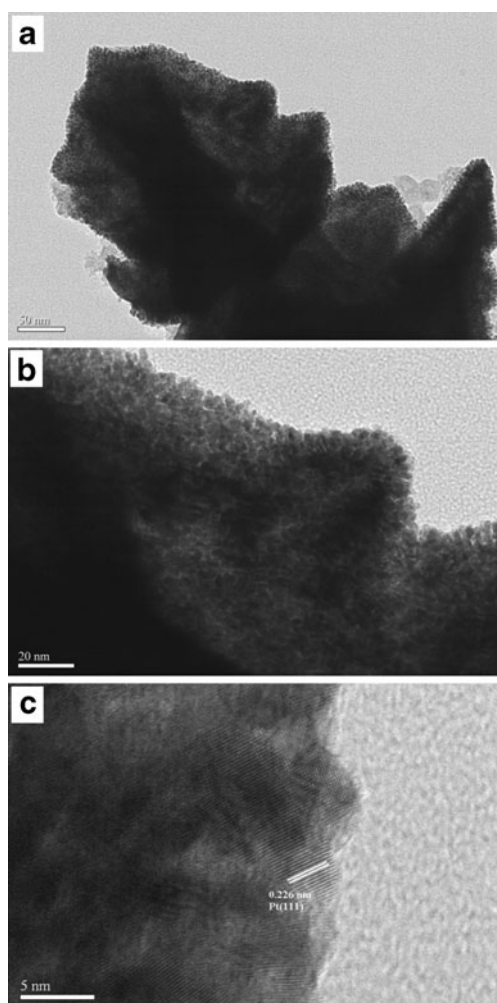ation of SEM that the branch of nanometer Au dendrites consisting of multilayer of nanometer pieces can perform the high ECA. After the Au/Si was dipped in H_2PtCl_6/HF electroless solution for 10 min, the dendrites does not become obvious, forming lots of pyramidal structure on Si substrate as shown in Fig. 1e,f, suggesting that the multilayer of the Au dendrites has been filled with the Pt particles. Fig. 1g shows the EDX pattern of Pt/Au/

Fig. 1 SEM image of composites: Pt/Si prepared in 3.5×10^{-3} M H_2PtCl_6+9.1 M HF solution for 10 min (**a**); Au/Si prepared in 4.4×10^{-3} M $HAuCl_4$+9.1 M HF for 10 min (**b**); Au/Si prepared in 4.4×10^{-3} M $HAuCl_4$+9.1 M HF for 30 min (**c**), (**d**); Pt/Au/Si prepared in 4.4×10^{-3} M $HAuCl_4$+9.1 M HF solution firstly for 30 min then in 3.5×10^{-3} M H_2PtCl_6+9.1 M HF solution for 10 min (**e**, **f**); EDX spectrum of Pt/Au/Si composites (**g**)
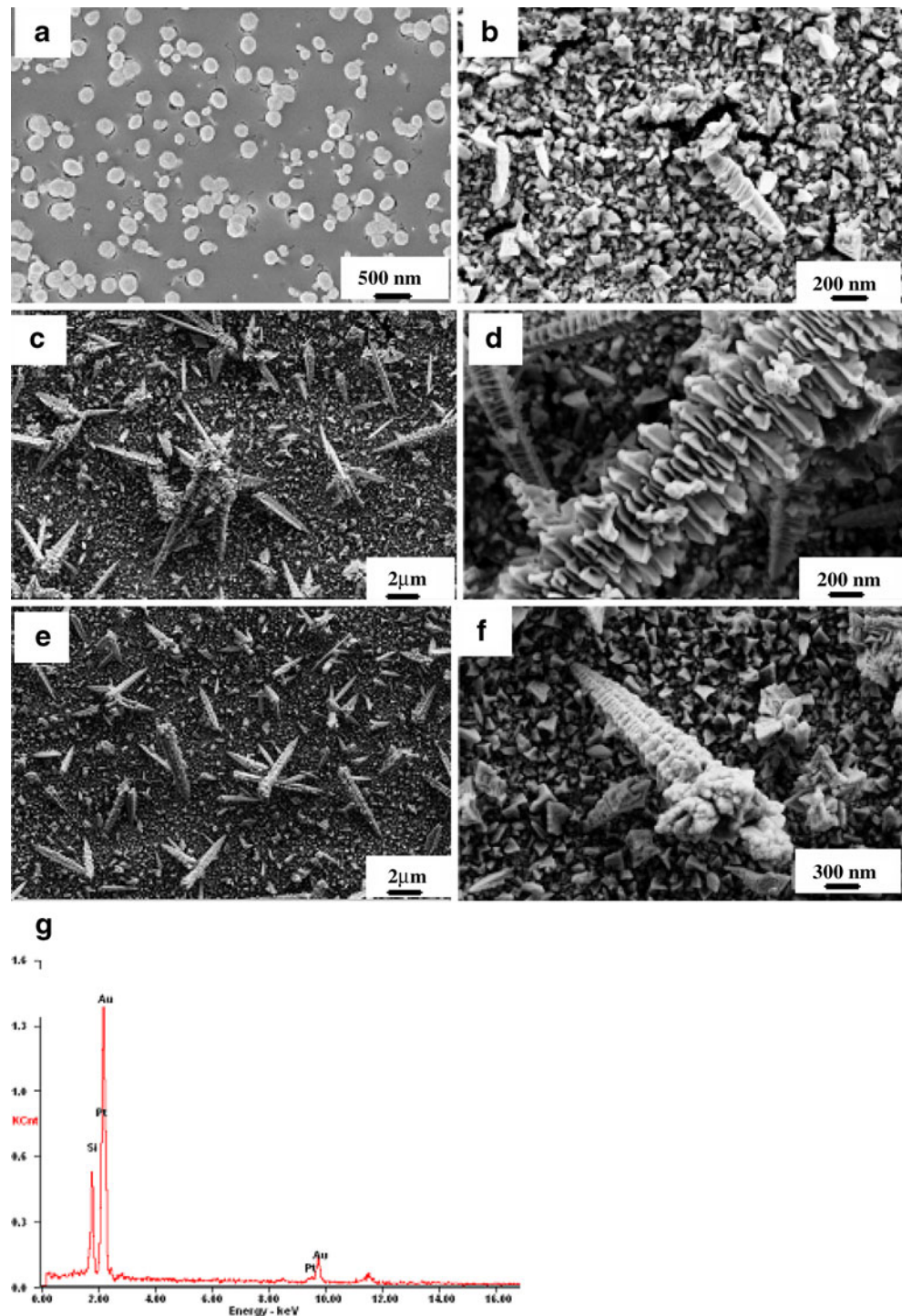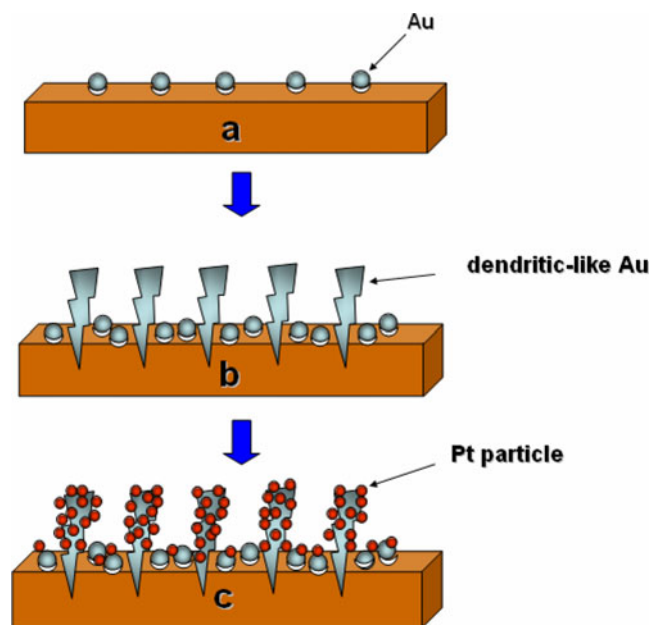
Si, the ratio of Au and Pt atomic element is 4.75:1, indicating that the Pt particles have been deposited on Au dendrites after being dipped into the H_2PtCl_6/HF electroless solution. This kind of Au structure can effectively disperse the distribution of Pt particles, offering a large ECA. Fig. 2 show the HR-TEM images of Pt/Au catalysts scratched from the Pt/Au/Si wafer. As can been seen from the figure, all the Pt particles appears to be well dispersed on the surface of branchs of Au and have a relatively narrow size of 3–5 nm. The further microstructure of the Pt catalyst was further examined by high-resolution of TEM measurement of Fig. 2c. As evidenced by the atomic features, the Pt nanoparticles are highly crystallized on the Au support. The 0.226 nm d-spacing is assigned to the Pt(111) [16].

The schematic mechanism of depositing Au and Pt particles on silicon can be described in Scheme 1. Firstly,
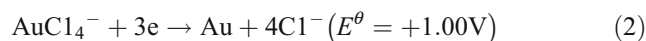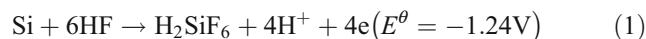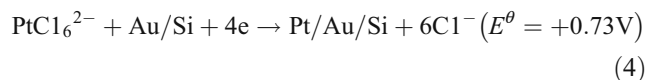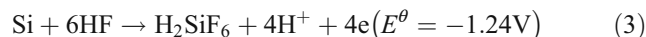
Scheme 1 Schematic mechanism of the formation of Pt/Au/Si catalyst

the nanoparticle of Au were deposited on silicon by the displacement reaction [17]:

$$Si + 6HF \rightarrow H_2SiF_6 + 4H^+ + 4e \left(E^\theta = -1.24V \right) \quad (1)$$

$$AuCl_4^- + 3e \rightarrow Au + 4Cl^- \left(E^\theta = +1.00V \right) \quad (2)$$

With the increase of deposition time, the Au nucleus grow rapidly, forming the Au dendrites with large active surface. After the prepared Au/Si was dipped in electroless H_2PtCl_6/HF solution, $PtCl_6^{2-}$ can get the electron from the Au dendrites or the silicon surface to which the oxidized Si releases, resulting in the deposition of Pt particles on dendritic Au and some Au particles. Accordingly, the Pt particles could be distributed on Au/Si. The reaction can be described as:

$$Si + 6HF \rightarrow H_2SiF_6 + 4H^+ + 4e \left(E^\theta = -1.24V \right) \quad (3)$$

$$PtCl_6^{2-} + Au/Si + 4e \rightarrow Pt/Au/Si + 6Cl^- \left(E^\theta = +0.73V \right) \quad (4)$$

The impact of Au/Si substrate prepared with different deposition time and concentration of $HAuCl_4$ on the electro-catalytic activity Pt/Au/Si were performed in Fig. 3a. The CV curves of Pt/Au/Si electrode after 100 cycles are performed as curve (a–c) and that of Pt/Si and Au/Si electrode is showed as curve (d) and (e), respectively.

Fig. 2 TEM images of Pt/Au catalysts. Pt/Au scratched from Pt/Au/Si prepared in 4.4×10^{-3} M $HAuCl_4$+9.1 M HF solution firstly for 30 min then in 3.5×10^{-3} M H_2PtCl_6+9.1 M HF solution for 10 min (**a**) and (**b**); high-resolution TEM images of **a** given by **c**

Fig. 3 Electrochemical measurements of: **a** CV curves of Pt/Au/Si and Pt/Si electrode in 1.0 M H_2SO_4, sweep rate:100 mVs^{-1}; **b** CV of Pt/Au/Si composites in 2 M CH_3OH+0.5 M H_2SO_4 solution, sweep rate: 100 mVs^{-1}, insert is the CV curves of Pt/Si in 2 M CH_3OH+0.5 M H_2SO_4 solution; **c** chronoamperometric curves of Pt/Au/Si and Pt/Si electrode in 2 M CH_3OH+0.5 M H_2SO_4 at 0.6 V; **d** CO stripping curves of Pt/Au/Si and Pt/Si electrode in CO saturated in 0.5 M H_2SO_4, sweep rate is 20 mVs^{-1}
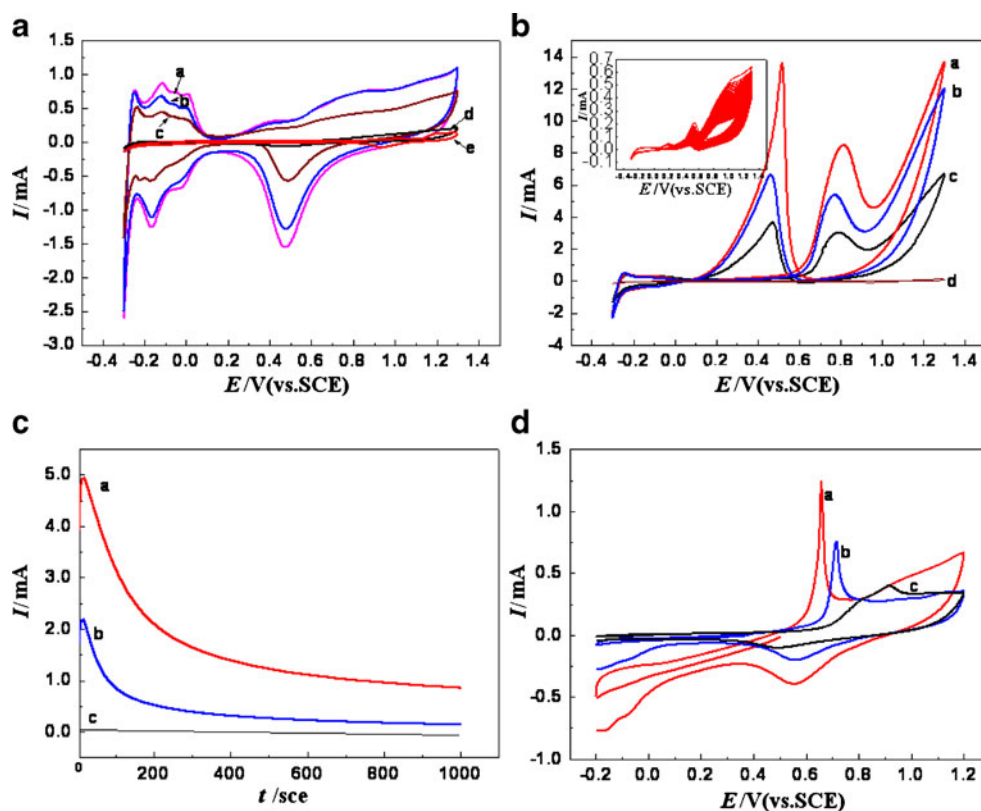
For curve (c), the Si was activated in lower concentration of 8.8×10^{-4} M $HAuCl_4$ for 10 min. While, for curve (a) and (b), silicon was plated in higher $HAuCl_4$ concentration of 4.4×10^{-3} M. Pt electroless deposition remained the same for curve of (a–d) within 10 min, suggesting the amount of deposited Pt is almost the same. As can be seen in curve (e), Au oxidation starts from 1.1 V and the reduction peak currents of oxidized gold is at about 0.9 V, indicating the Au particles have been deposited on Si surface and the Au/Si electrode is stable in the acid solution. The real electrochemical surface area of Pt/Au/Si could be obtained from integrated charge in hydrogen absorption or desorption region of cyclic voltammogram. A value generally admitted for ploycrystalline Pt electrode and Pt loading [18].

EAS($m^2 g^{-1}$Pt)=Q_H/(0.21×10^{-3}Cg^{-1}Pt), where EAS is the electrochemically active surface of Pt particles obtained electrochemically, Q_H is the amount of charge exchanged during the electrodesorption.

It can be seen that the Pt/Si catalyst show poorly resolved peak of hydrogen adsorption and desorption in the potential region −0.3 to 0 V (curve d) with the desorption charge Q_H=0.116 $mCcm^{-2}$ and EAS=1.06 $m^2 g^{-1}$, suggesting that Pt/Si electrode has the very low EAS. While, two peaks of hydrogen adsorption were clearly observed from −0.2 to 0 V in curve (a–c), showing the characterized curves of polycrystalline Pt in H_2SO_4 solution. In comparison with

curve (a, b) in Fig. 3a, with the increased time of Au activation, Pt/Au/Si with Au activation for 30 min exhibits broader peak (Q_H=7.32 $mCcm^{-2}$ and EAS=69.4 $m^2 g^{-1}$) higher than that of Pt/Au/Si with Au activation for 10 min (Q_H=5.62 $mCcm^{-2}$ and EAS=53.3 $m^2 g^{-1}$). This indicate that longer Au activation time would favor the higher electrochemical surface area, offering the larger active surface area for Pt particle to deposit. The distribution of Pt particles on Au nuclei could also be increased with longer activation time. The concentration of $HAuCl_4$ also has the strong effect on the catalytic properties of Pt/Au/Si electrode. By comparsion with curve (b) and (c) of Fig. 3a, with the concentration of $HAuCl_4$ decreased from 4.4×10^{-3} to 8.8×10^{-4} M, the peak of hydrogen adsorption and desorption reduce for the desorption charge Q_H is 3.36 $mCcm^{-2}$ and EAS is 31.8 $m^2 g^{-1}$, suggesting the lower concentration of $HAuCl_4$ will reduce the active surface area of Au/Si and the distribution of Pt particles will also be reduced as well. Accordingly, the values indicate that the higher electrochemical surface area could be obtained by increase of Au activation time and concentration of $HAuCl_4$.

Figure 3b shows the CV curves after 100 cycle of methanol electrooxidation. Pt/Au/Si catalysts were prepared by electroless deposition of Pt for 10 min on Au/Si substrates activated in 4.4×10^{-3} M $HAuCl_4$/9.1 M HF for 30 and 10 min for curve (a,b) and in 8.8×10^{-4} M $HAuCl_4$/9.1 M HF

for 10 min for curve (c), respectively. Insert is the CV curves of Pt/Si in 2 M CH_3OH+0.5 M H_2SO_4 solution. The current, much lower than that of Pt/Au/Si, decreases from outer to inner as the CV circles increase, indicating Pt particles can be easily detached from silicon wafer in the case of the poor adhesion in acid solution, which cannot easily present the excellent the electro-catalytic activity for methanol due to its poor durability in low concentration of H_2PtCl_6 [19]. Compared with curve (a) and (b), the catalyst of Pt on Au dendrites activated for 30 min (curve a) presents higher methanol oxidation current than that of Au/Si activated for 10 min (curve b). With the different Au^{3+} concentration but same time activation of Au^{3+}, curve (b) shows the higher methanol oxidation current than that of curve (c). The curve (d) is the CV feature of Au/Si electrode for methanol electrooxidaton. As can be seen that oxidation peak at 1.1v can be assigned as the oxidation of Au, indicating that Au/Si has the no electrocatalytic activity for methanol in acid solution and the increased current of methanol oxidation of curve (a, b, c) can be fully related to the Pt catalyst deposited on Au/Si substrate. Accordingly, with growth of Au dendrites, the distribution to the same amonut of Pt on Au/Si would be highly enhanced on Au dendrites with large active area and its electrooxidation activity would be increased as the result. These are fully consistent with the CV measurements shown in Fig. 3a.

The chronoamperometry tests in 2.0 M CH_3OH/0.5 M H_2SO_4 at 0.6 V for 1,000 s were performed in Fig. 3c. The potential step from the open circuit potential to 0.6 V was applied immediately after introducing the electrode to the solution. For curve (a), (b), and (c), the potentiostatic current is gradually decayed for both the catalysts due to the formation of intermediate species, such as CO_{ads}, CH_3OH_{ads}, and CHO_{ads} during the methanol oxidation reaction [19]. It can be seen that the potentiostatic currents of Pt/Au/Si electrodes (curve a, b) are higher than that of Pt/Si electrode (curve c) and the potentiostatic currents of curve (b) decrease more rapidly than that of curve (a), indicting Pt/Au/Si electrodes are more active than Pt/Si electrode for methanol electrooxidation and the longer Au^{3+} activation time will result in the higher stability and higher specific area, which aggree well with the CV results.

To compare the CO tolerance of dendritic-like Pt/Au/Si and Pt/Si electrode, CO-stripping CV measurement was carried out. Fig. 3d shows the CV curves of CO stripping in 0.5 M H_2SO_4 solution. Curve (c) is for Pt/Si electrode. Curve (a) and (b) is Pt/Au/Si electrode acitvated in 4.4×10^{-3} M $HAuCl_4$/9.1 M HF solution for 30 and 5 min, respectively. CO oxidation went to completion in the first scan with no trace of CO after that. The peak current density of CO electrooxidation on Pt/Au/Si is much larger than that of Pt/Si. The Pt/Au/Si electrode with Au^{3+} activation for 30 min shows larger CO oxidation current

than that of 5 min Au^{3+} activation, further indicating that Pt/Au/Si electrode has much larger electrochemically active area and the Pt could be distributed on Au/Si with the increased time of Au^{3+} activation. It is clear to see that the CO oxidation peak potential of Pt/Au/Si is at 0.71 and 0.66 V with the Au^{3+} activation for 5 and 30 min, respectively, much lower than that of Pt/Si at 0.91 V. This suggest that Pt/Au/Si electrode is much easier to oxidize the CO than that of Pt/Si catalyst and Pt/Au/Si electrode shows greater ease of CO removal with the increase of Au^{3+} activation time. The facile removal of CO on Pt/Au/Si to Pt/Si reflects the effectiveness of the interface between thin Pt shell and the underlying dendritic Au [20]. The Pt/Si interface is not effective in contributing to the removal of adsorbed CO. The active oxygen-containing species on the neighboring sites play a key role in the oxidative removal of CO_{ads}. By using XPS measurement, Zeng et al. [21] found that electron transfer from Au to Pt additionally enhanced oxygen presence on the catalyst surface in the case of Au/Pt. The higher Pt oxide content as the acitvate type in the Au core Pt shell system, facilitating CO_{ads} removal, appears to correlate well with the presence of Au. Fig. 3d also shows that reduction current of Pt oxide is higher in the case of longer Au^{3+} activation time, confirming more extensive presence of active oxygen-contaning species on Pt/Au/Si interface with the increase of Au active surface.

The electrochemical impedance spectroscopy is the effective way to measure the charge–transfer resistance and capacitance of the electrode during the methanol electrooxidation [5]. Figure 4 shows complex impedance plots measured in 2 M CH_3OH/0.5 M H_2SO_4 aqueous solution in a potentiostatic mode of 0.3 V (vs. SCE), where
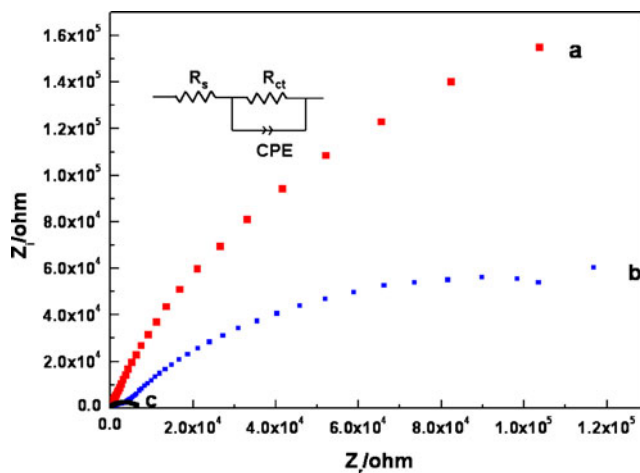
Fig. 4 Complex impedance plots measured in 2 M CH_3OH+0.5 M H_2SO_4 Au/Si composites prepared in 4.4×10^{-3} M $HAuCl_4$+9.1 M HF solution for 30 min (a), Pt/Si prepared in 3.5×10^{-3} M H_2PtCl_6+9.1 M HF solution for 10 min (b), Pt/Au/Si composites firstly prepared in 4.4×10^{-3} M $HAuCl_4$+9.1 M HF solution for 30 min then in 3.5×10^{-3} M H_2PtCl_6+9.1 M HF solution for 10 min (c)

Z_r and Z_i represent the real and imaginary components of the impedance, respectively. The equivalent circuit model shown in the inset of Fig. 4 was used to fit the experimental data. The R_s resistor is the resistance of the electrolyte solution, R_{ct} is the charge transfer resistance of the electrolyte solution and CPE represents the constant phase element [5, 22]. The Nyquist plots consist mainly of semicircles, whose diameters are associated with the charge transfer resistance indicating the catalytic activity for methanol oxidation reaction [23]. The shrinkage in diameter of semicircles in Nyquist plots reflects the improved catalytic activities toward methanol. By comparison, it can be seen that the diameter of the semicircle for Au/Si has the largest diameter of the semicircle, while that of Pt/Si is slightly smaller, Pt/Au/Si shows the smallest diameter of the semicircle in CH_3OH/H_2SO_4 solution, demonstrating Pt/Au/Si has the very low R_{ct} far more excellent electro-oxidation activity than that of Pt/Si and Au/Si electrode.

Conclusions

In summary, the Pt/Au/Si catalysts with large ECA were successfully synthesized via a new time-saving EDD method. A high dispersion of Pt particles on three-dimensional dendritic Au supported on Si wafer were obtained. The Pt/Au/Si catalysts show much higher electro-catalytic activity and stability than that of Pt/Si composite. It was found that the three-dimensional dendritic Au play an important role for the distribution of Pt particles. The Au dendrites enhanced the distribution of Pt particles, leading to the higher electro-catalytic properties toward methanol and CO oxidation. The anodic CO peak of Pt/Au/Si catalyst showed negatively shifted with respect to similarly prepared Pt/Si electrode. The method is simple, time-saving, and easy to control. Therefore, it is expected to have potential for the preparation of commercial catalysts. The approach may be useful for the synthesis of other metal/Au/Si catalysts.

References

1. Shao MH, Shoemaker K, Peles A, Kaneko K, Protsailo L (2010) J Am Chem Soc 132:9253
2. Zhao D, Xu BQ (2006) Angew Chem Int Ed 45:4955
3. Spiegel RJ (2004) Transp Res 9:357
4. Ge XB, Yan XL, Wang RY, Tian F, Ding Y (2009) J Phys Chem C 113:7379
5. Tiwari JN, Pan FM, Tiwari RN, Nandi SK (2008) Chem Commun 48:6516
6. Wang CH, Sun DC, Xia XH (2006) Nanotechnol 17:651
7. Tiwari JN, Pan FM, Lin KL (2009) New J Chem 33:1482
8. Tong H, Zhu L, Li MK, Wang CM (2003) Electrochim Acta 48:2473
9. Yae S, Nasu N, Matsumoto K, Hagihara T, Fukumuro N, Matsuda H (2007) Electrochim Acta 53:35
10. Rosa CP, Iglesia E, Maboudian R (2009) Electrochim Acta 54:3270
11. Peng KQ, Yan YJ, Gao SP, Zhu J (2003) Adv Funct Mater 13:127
12. Peng KQ, Zhu J (2004) Electrochim Acta 49:2563
13. Munoz EC, Schrebler RS, Grez PC, Henriquez RG, Heyser CA, Verdugo PA, Marotti RE (2009) J Electroanal Chem 633:113
14. Shao MH, Adzic RR (2005) Electrochim Acta 50:2415
15. Tong H, Wang CM (2002) Acta Chim Sinica 60:1923
16. Zhang Y, Huang QH, Zou ZQ, Yang JF, Vogel W, Yang H (2010) J Phys Chem C 114:6860
17. Magagnin L, Maboudian R, Carraro C (2002) J Phys Chem B 106:401
18. Tong H, Li HL, Zhang XG (2007) Carbon 45:2424
19. Gorostiza P, Allongue P, Díaz R, Morante JR, Sanz FJ (2003) J Phys Chem B 107:6454
20. Song HQ, Qiu XP, Guo DJ, Li FS (2008) J Power Sources 178:97
21. Zeng JH, Jun Y (2006) J Phys Chem B 110:24606
22. Koczkur K, Yi Q, Chen A (2007) Adv Mater 19:2648
23. Guo DJ, Cui SK (2009) J Colloid Interface Sci 340:53